Electronic Supplementary Information

Probing promotional effects of potassium and the nature of active chromium species in Cr/MCM-41 catalysts for methyl mercaptan abatement

Yutong Zhao[a], Jichang Lu[a], Dingkai Chen[a], Liming Zhang[a], Sufang He[b], Caiyun Han[a], Dedong He*[c], Yongming Luo*[a]

[a] Faculty of Environmental Science and Engineering, Kunming University of Science and Technology, Kunming 650500, PR China.

[b] Research Center for Analysis and Measurement, Kunming University of Science and Technology, Kunming, 650093, PR China.

[c] Faculty of Chemical Engineering, Kunming University of Science and Technology, Kunming 650500, PR China.

* Corresponding author

Tel: +86-871-65103845

Fax: +86-871-65103845

E-mail: dedong.he@qq.com;

environcatalysis222@yahoo.com

2 Experimental

2.1 Synthesis of support and catalysts

MCM-41 was synthesized via hydrothermal method by employing tetraethyl orthosilicate (TEOS) as silicon source and cetyltrimethyl ammonium bromide (CTAB) as the template. Ammonium solution (NH_4OH) was used to adjust the pH of synthesis solution. In a typical synthesis batch, 14 g of CTAB and 54 mL of NH_4OH were dissolved into 635 mL of deionized water under ambient temperature. Next to, 57.6 mL of TEOS was introduced by dripping in the above mixture solution under continuous stirring. Subsequently, the white solid was obtained after filtrated and dried 110 ^oC for 24 h. Finally, the sample was calcined under 550 ^oC for 5 h.

MCM-41 supported Cr-based catalysts were prepared via incipient wetness impregnation route, and the corresponding procedures were registered as follows: the calculated amount of Cr precursors ($H_8CrN_2O_4$, $K_2Cr_2O_7$ and K_2CrO_4) was added to hot deionized water to ensure that the precursor was completely dissolved so as to keep the same loading of Cr. Next to, 2 g of MCM-41 was rapidly added into the above mixture solution so as to make all the liquid to be totally adsorbed by MCM-41. Almost immediately, the resulted sample was placed under ambient temperature for one night, then dried at 110 ^oC for 6h. Finally, the dried material was calcined under 550 ^oC for 5h in air. The corresponding samples prepared with $H_8CrN_2O_4$, $K_2Cr_2O_7$ and K_2CrO_4 were denoted as Cr-N/MCM-41, Cr-K/MCM-41 and Cr-K_2/MCM-41, respectively.

To investigate and understand the roles of K addition, two other materials were also synthesized by using incipient wetness impregnation. The first one was named as K/MCM-41 that was prepared according to the above synthesis procedures by replacing Cr precursor with K_2CO_3. The second one was labelled as Cr-N-K/MCM-41, in which Cr-N/MCM-41 rather than MCM-41 was impregnated with K_2CO_3, and the mole ratio of Cr to K was kept at 1.0(Cr/K = 1.0). Moreover, to determine the optimum Cr content and K content on active Cr-N-K/MCM-41 sample, the different mole ratio of xCr-N-yK/MCM-41 catalysts (x=0.5, y=1; x=1.5, y=1; x=1, y=0.5; x=1, y=1.5) were also prepared at Cr/K =0.5, 1.5 and K/Cr=0.5, 1.5 by using incipient wetness impregnation.

The mechanically mixed catalysts (i.e. CrO_3/MCM-41, Cr_2O_3/MCM-41 and CrO_3+Cr_2O_3/MCM-41) containing 18 wt % Cr loading were synthesized. CrO_3+Cr_2O_3/MCM-41 catalyst was prepared by mixing equal masses of each component by means of grinding. Then, the obtained catalyst followed by calcination at 300 ^oC for 5h in N_2.

2.2 Catalyst characterization

X-ray diffraction (XRD) patterns of catalyst samples were recorded on a Rigaku D/max - 1200 diffractometer by using Cu Kα radiation (λ=1.5406 Å) within the scattering angle (2θ) range of 20-80°. The spectra of Ultraviolet-visible (UV-vis) diffuse reflectance were obtained from a PERSEE TU-1901 and tested in the region of 250-800 nm at room temperature. X-ray photoelectron spectroscopy (XPS) was implemented on a PHI 5000 Versa Probe II spectrometer by using non-monochromatic Al Kα radiation (1486.6 eV) as X-ray source and photoelectron peak of C1s (284.6 eV) was employed to adjust binding energy for reference. Thermogravimetric (TG) analysis was carried out on a Mettler-Toledo TGA/DSC (STA449F3) instrument, and the sample was heated from 50 to 800 ^oC (10 ^oC/min) within nitrogen (N_2) flow. Chromium and potassium content of the samples were determined by ICP-OES.

The profiles of temperature-programmed reduction of hydrogen (H_2-TPR) were recorded on a fixed-bed reactor at temperature range from 200 ^oC to 700 ^oC. Firstly, 50 mg of catalyst was pre-treated at 400 ^oC for 1h by using the flow of 5 vol% O_2 in argon (Ar) to eliminate some physisorbed species on the surface of sample so as to keep the same conditions. After that, the obtained material were cooled to 200 ^oC within the ultra-pure argon (Ar) flow. Subsequently, H_2-TPR test was performed under the 10% H_2/Ar (30 cm^3/min) with the heating rate of 10 ^oC/min from 200 ^oC to 700 ^oC, and hydrogen (H_2) consumption during the reduction reaction process was monitored by an on-line thermal conductivity detector (TCD).

Base properties of catalyst samples were characterized by CO_2-TPD, in which a TCD was used to on-line detect the concentration of the desorbed carbon dioxide (CO_2). Before CO_2-TPD experiment, the catalyst (100 mg) was treated with helium (He, 30 cm^3/min) flow at 500 °C for 2 h, then the obtained catalyst was cooled to room temperature. After that, the catalyst was saturated by 10% CO_2 within He (30 cm^3/min) under room temperature. Then, the saturated catalyst were purified at 100 °C with ultra-pure helium (He) gas for 1 h to remove weak CO_2 and/or physically adsorbed CO_2. CO_2-TPD profile was recorded by heating cell temperature from 100 to 800 °C in ramp rate of 10 °C/min within ultra-pure He (30 cm^3/min). O_2-TPD were tested by similar experimental method on the same apparatus equipped with TCD. The catalysts (100 mg) were first treated at 450 °C for 1h in He flow (30 cm^3/min) and cooled to room temperature in the same atmosphere, then O_2 (oxygen) flow was continuously pass at 30 cm^3/min though materials for 1h. Then the saturated sample were swept using flowing He. O_2-TPD profile was carried out at a heating rate of 10 °C/min from 30 to 800 °C in flowing He.

2.3 Catalytic activity test

The catalytic activity tests for CH_3SH decomposition was measured in a fixed-bed micro-reactor under atmospheric pressure at temperature region between 250 ^oC and 500 ^oC. 0.2g of catalyst with 60-40 mesh size was placed in the reactor. Then, the reactant gas mixture (1% CH_3SH balanced with N_2) in total flow 30 cm^3/min was introduced to the reaction system. The outlet gas from the reactor was analyzed by employing two sets of on-line GC equipped with a flame photometric detector (FPD), a thermal conductivity detector (TCD), two flame ionization detectors (FID) together with one methanation reactor.

The conversion of CH_3SH (%) is defined as:

$$CH_3SH\ conversion = \frac{C_{(CH_3SH)in} - C_{(CH_3SH)out}}{C_{(CH_3SH)in}} \times 100\%$$

$C_{(CH3SH)in}$ represents the CH_3SH initial concentration, and $C_{(CH3SH)out}$ denotes the CH_3SH residual concentration after reaction.

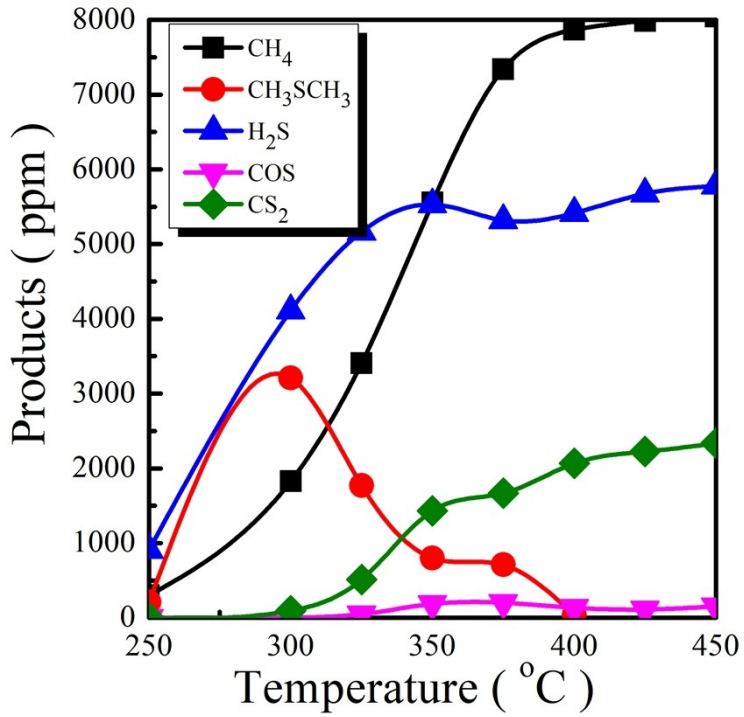

Figure S1. Decomposition products as a function of reaction temperature on Cr-N/MCM-41.

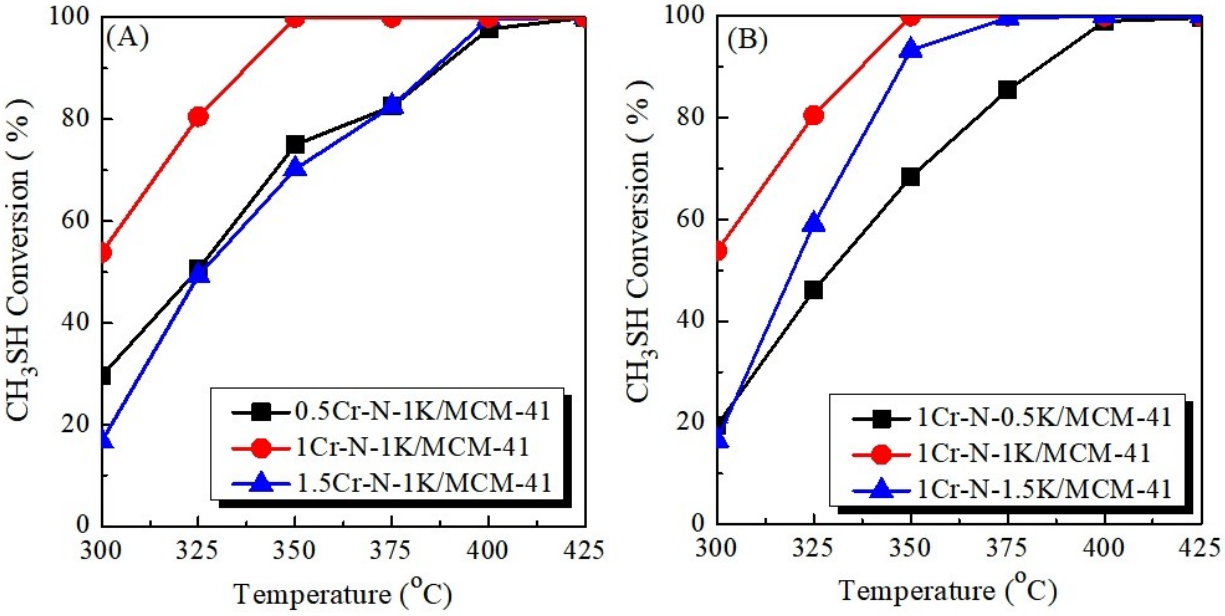

Figure S2. Conversion of CH_3SH as a function of reaction temperature on different Cr to K molar ratio of Cr-N-K/MCM-41 catalysts

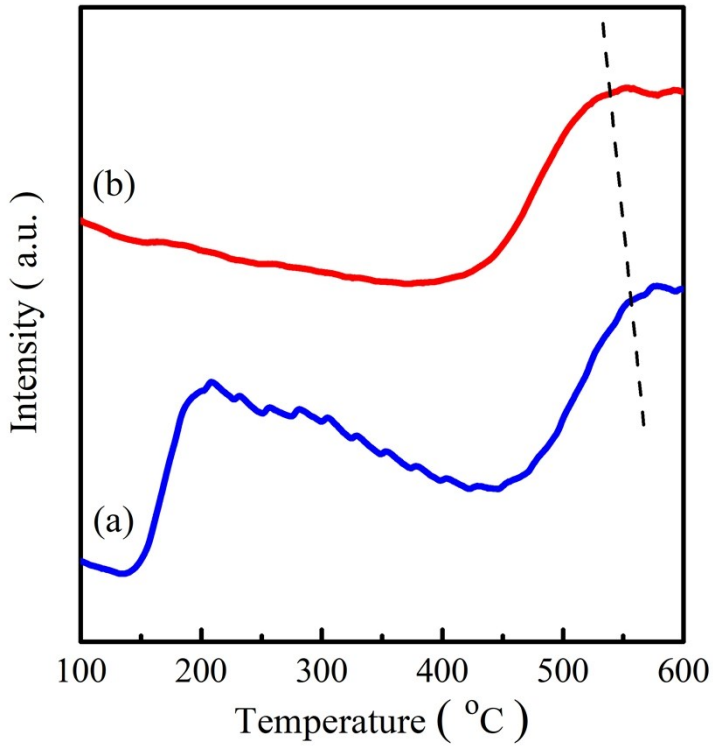

Figure S3. NH_3-TPD profiles of (a) Cr-N/MCM-41 and (b) Cr-N-K/MCM-41 catalysts.

With the addition of K, the intensity of weak acid sites decreased and the temperature of strong acid peak shift to the lower temperature. This phenomenon proves that alkali metal potassium significantly reduces the acidity of Cr-N/MCM-41 sample, which is beneficial to the catalytic conversion CH_3SH

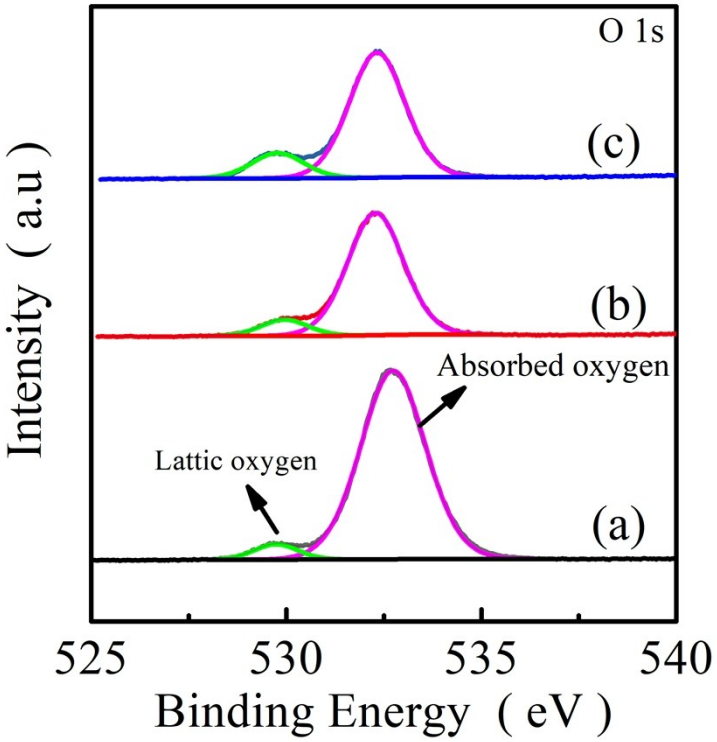

Figure S4. XPS of O 1s of (a) Cr-N/MCM-41, (b) Cr-K/MCM-41 and (c) Cr-N-K/MCM-41.

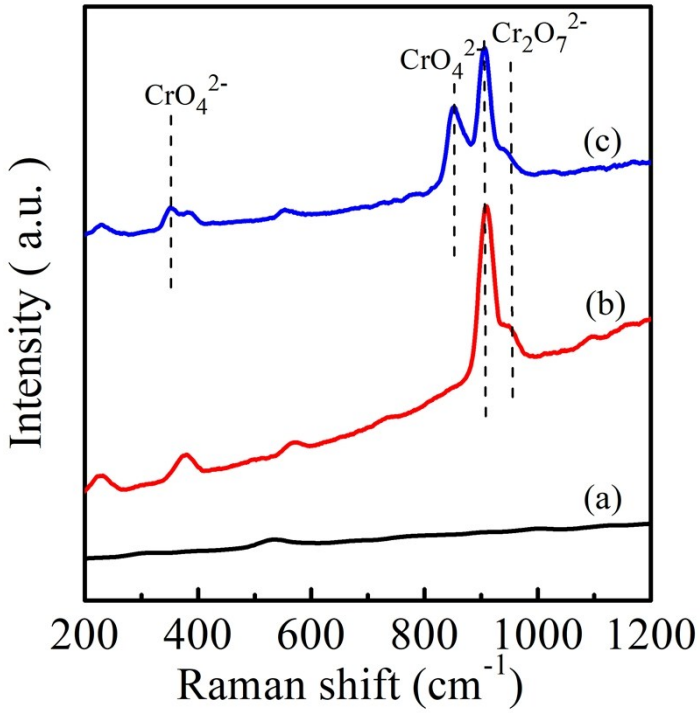

Figure S5. Raman spectra of (a) Cr-N/MCM-41, (b) Cr-K/MCM-41 and (c) Cr-N-K/MCM-41.

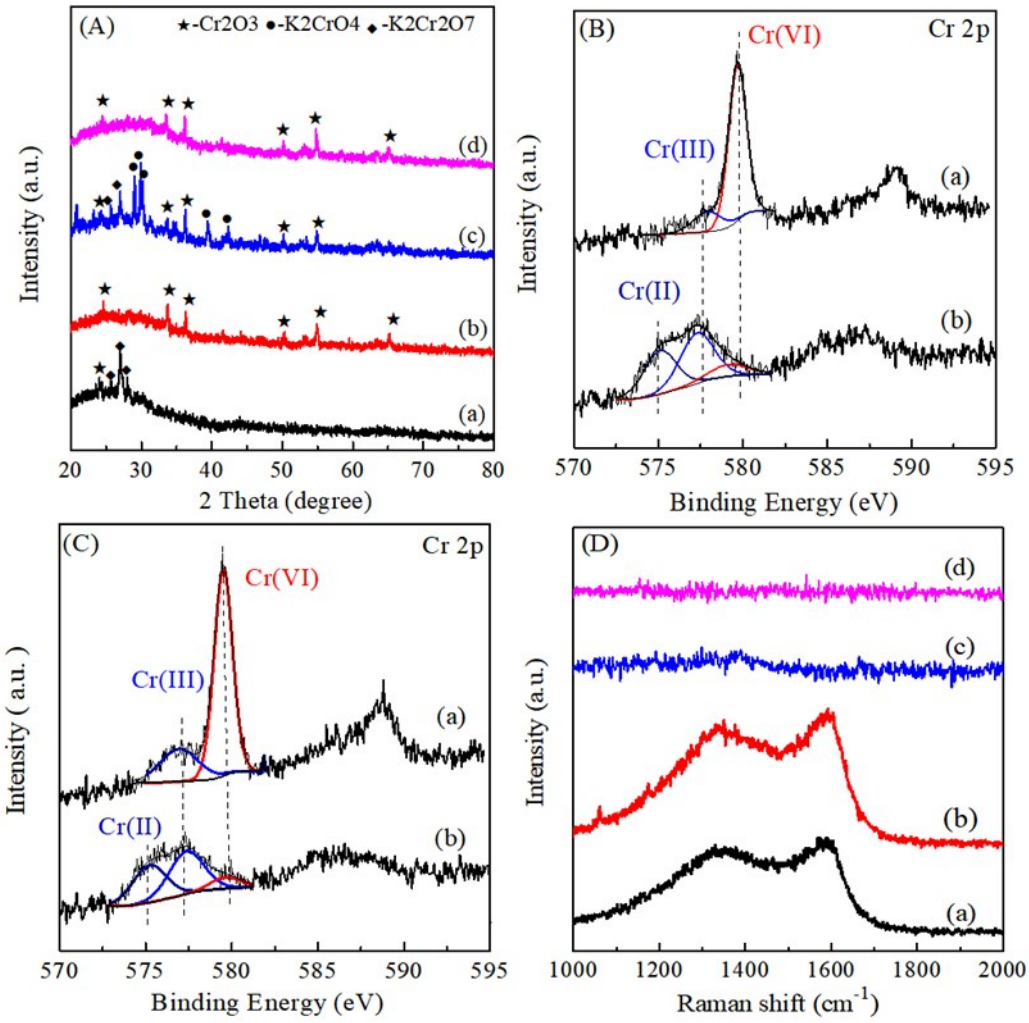

Figure S6. (A) XRD patterns of K-containing catalysts: (a) Fresh Cr-K/MCM-41; (b) Spent Cr-K/MCM-41; (c) Fresh Cr-N-K/MCM-41; (d) Spent Cr-N-K/MCM-41. (B) XPS spectra of fresh (a) and spent (b) Cr-K/MCM-41 catalyst. (C) XPS spectra of fresh (a) and spent (b) Cr-N-K/MCM-41 catalyst. (D) Raman spectra of spent and regenerated catalysts: (a) Spent Cr-K/MCM-41; (b) Spent Cr-N-K/MCM-41; (c) Regenerated Cr-K/MCM-41; (d) Regenerated Cr-N-K/MCM-41.

Table S1 ICP-OES results on different Cr to K molar ratio of Cr-N-K/MCM-41 samples.

Sample	Cr/K	ICP-OES		
		K content (%)	Cr content (%)	Cr/K (ICP)
0.5Cr-N-1K/MCM-41	0.5	11.9	6.4	0.54
1Cr-N-1K/MCM-41	1	11.9	10.7	0.90
1.5Cr-N-1K/MCM-41	1.5	11.9	14.1	1.18

Table S2 ICP-OES results on different K to Cr molar ratio of Cr-N-K/MCM-41 samples.

Sample	K/Cr	ICP-OES		
		K content (%)	Cr content (%)	Cr/K (ICP)
1Cr-N-0.5K/MCM-41	0.5	6.08	10.5	0.58
1Cr-N-1K/MCM-41	1	11.9	10.7	1.11
1Cr-N-1.5K/MCM-41	1.5	17.3	10.1	1.71

Table S3 Catalytic activity comparison of K-containing with other reported catalyst

Catalyst	Temperature(^{o}C) [a]	Refs.
CeO_2	450	[1]
$Ce_{0.75}Y_{0.25}O_2$	450	[2]

HZSM-5	550	[3]
Cr/ZSM-5	450	[4]
Nd/ZSM-5	500	[5]
Sm/ZSM-5	500	[6]
La/ZSM-5	500	[3]
Reused Cr adsorbent	400	[7]
Cr-N/MCM-41	450	Present work
Cr-K/MCM-41	375	Present work
Cr-N-K/MCM-41	350	Present work

Table S4 Thermodynamic data (ΔH, S, G, K_p and $Log_{10}(K_p)$) of equation (1) obtained from HSC Chemistry software under various temperature.

Reactions	**$4(NH_4)_2CrO_4 = 2CrO_3 + Cr_2O_3 + N_2$ (g) + $6NH_3$ (g) + $7H_2O$ (g) (1)**														
	0 °C	50 °C	100 °C	150 °C	200 °C	250 °C	300 °C	350 °C	400 °C	450 °C	500 °C	550 °C	600 °C	650 °C	700°C
$\Delta H_r(T)$ (kJ/mol)	111.415	120.845	130.638	140.735	158.309	169.314	180.515	191.894	203.453	215.193	227.113	239.210	251.483	263.929	276.548
$\Delta S_r(T)$ (J/K/mol)	535.433	567.103	595.273	620.657	659.149	681.255	701.701	720.734	738.575	755.397	771.334	786.494	800.967	814.828	828.139
$\Delta G_r(T)$ (kJ/mol)	-34.839	-62.415	-91.488	-121.896	-153.567	-187.085	-221.665	-257.231	-293.719	-331.072	-369.244	-408.192	-447.882	-488.279	-529.355
K_p	4.601E+006	1.229E+010	6.424E+012	1.118E+015	9.013E+016	4.801E+018	1.597E+020	3.663E+021	6.218E+022	8.242E+023	8.881E+024	8.032E+025	6.251E+026	4.272E+027	2.606E+028
$Log_{10}(K_p)$	6.663	10.090	12.808	15.048	16.955	18.681	20.203	21.564	22.794	23.916	24.948	25.905	26.796	27.631	28.416

Table S5 Thermodynamic data (ΔH, S, G, K_p and $Log_{10}(K_p)$) of equation (2) obtained from HSC Chemistry software under various temperature.

Reactions	**$2K_2Cr_2O_7 = 2K_2O + 2Cr_2O_3 + 3O_2(g)$ (2)**													
	0 °C	50 °C	100 °C	150 °C	200 °C	250 °C	300 °C	350 °C	400 °C	450 °C	500 °C	550 °C	600 °C	650 °C	700°C
$\Delta H_r(T)$ (kJ/mol)	527.971	539.612	551.414	563.266	575.413	587.926	600.770	614.775	632.295	645.897	659.573	673.316	687.120	700.981	714.896
$\Delta S_r(T)$ (J/K/mol)	174.178	213.246	247.209	277.008	304.136	329.269	352.713	376.148	403.219	422.710	440.996	458.219	474.499	489.936	504.615
$\Delta G_r(T)$ (kJ/mol)	480.395	470.702	459.168	446.050	431.512	415.669	398.613	380.378	360.868	340.215	318.617	296.133	272.811	248.697	223.830
K_p	1.337E-092	8.099E-077	5.235E-065	8.590E-056	2.281E-048	3.115E-042	4.666E-037	1.296E-032	9.891E-029	2.652E-025	2.966E-022	1.610E-019	4.767E-017	8.449E-015	9.655E-013
$Log_{10}(K_p)$	-91.874	-76.092	-64.281	-55.066	-47.642	-41.507	-36.331	-31.887	-28.005	-24.576	-21.528	-18.793	-16.322	-14.073	-12.015

Table S6 Thermodynamic data (ΔH, S, G, K_p and $Log_{10}(K_p)$) of equation (3) obtained from HSC Chemistry software under various temperature.

Reactions	**$2\ Cr_2O_3 + 4K_2CO_3 + 3O_2\ (g) = 4K_2CrO_4 + 4CO_2\ (g)$ (3)**														
	0 °C	50 °C	100 °C	150 °C	200 °C	250 °C	300 °C	350 °C	400 °C	450 °C	500 °C	550 °C	600 °C	650 °C	700°C
$\Delta H_r(T)$ (kJ/mol)	-156.246	-157.444	-158.486	-159.463	-160.720	-162.366	-164.379	-166.669	-169.221	-174.949	-175.492	-175.747	-175.668	-175.209	-156.459
$\Delta S_r(T)$ (J/K/mol)	129.513	125.532	122.520	120.068	117.269	113.968	110.297	106.469	102.533	94.258	93.530	93.209	93.300	93.809	113.848
$\Delta G_r(T)$ (kJ/mol)	-191.622	-198.009	-204.205	-210.270	-216.205	-221.988	-227.596	-233.015	-238.241	-243.112	-247.805	-252.472	-257.133	-261.809	-267.250
K_p	4.437E+036	1.022E+032	3.869E+028	9.086E+025	7.422E+023	1.467E+022	5.545E+020	3.418E+019	3.079E+018	3.647E+017	5.537E+016	1.053E+016	2.420E+015	6.534E+014	2.218E+014
$Log_{10}(K_p)$	36.647	32.009	28.588	25.958	23.871	22.167	20.744	19.534	18.488	17.562	16.743	16.022	15.384	14.815	14.346

Table S7 Thermodynamic data (ΔH, S, G, K_p and $Log_{10}(K_p)$) of equation (4) obtained from HSC Chemistry software under various temperature.

Reactions	**$4K_2CrO_4 + 2\ Cr_2O_3 + 3O_2\ (g) = 4K_2Cr_2O_7$ (4)**														
	0 °C	50 °C	100 °C	150 °C	200 °C	250 °C	300 °C	350 °C	400 °C	450 °C	500 °C	550 °C	600 °C	650 °C	700°C
$\Delta H_r(T)$ (kJ/mol)	-53.434	-64.740	-76.389	-88.239	-100.375	-112.821	-125.559	-138.561	-151.843	-165.426	-179.327	-193.566	-208.164	-223.144	-247.458
$\Delta S_r(T)$ (J/K/mol)	-84.247	-122.208	-155.720	-185.515	-212.618	-237.617	-260.868	-282.614	-303.114	-322.576	-341.161	-359.004	-376.219	-392.899	-418.677
$\Delta G_r(T)$ (kJ/mol)	-30.422	-25.249	-18.282	-9.738	0.225	11.489	23.958	37.550	52.198	67.844	84.441	101.948	120.331	139.561	159.978
K_p	**6.578E+005**	**1.207E+004**	**3.626E+002**	**1.593E+001**	**9.444E-001**	**7.125E-002**	**6.553E-003**	**7.114E-004**	**8.896E-005**	**1.256E-005**	**1.971E-006**	**3.389E-007**	**6.321E-008**	**1.266E-008**	**2.584E-009**
$Log_{10}(K_p)$	5.818	4.082	2.559	1.202	-0.025	-1.147	-2.184	-3.148	-4.051	-4.901	-5.705	-6.470	-7.199	-7.897	-8.588

References

[1] D. He, G. Wan, H. Hao, D. Chen, J. Lu, L. Zhang, F. Liu, L. Zhong, S. He, Y. Luo, Chem. Eng. J., 2016, 289, 161-169.
[2] D. Chen, D. Zhang, D. He, J. Lu, L. Zhong, C. Han, Y. Luo, Chin. J. Catal, 2018, 39:1929-1941.
[3] J. Lu, H. Hao, L. Zhang, Z. Xu, L. Zhong, Y. Zhao, D. He, J. Liu, D. Chen, H. Pu, S. He, Y. Luo, Appl. Catal. B, 2018, 237, 185-197.
[4] D. He, J. Yu, Y. Mei, J. Liu, Y. Zhao, S. Yang, X. Cao, S. He, Y. Luo, Catal. Commun.,2018, 112, 31-34.
[5] D. He, H. Hao, D. Chen, J. Liu, J. Yu, J. Lu, F. Liu, S. He, K. Li, Y. Luo, Appl. Catal. A Gen., 2017, 533, 66-74.
[6] D. He, D. Chen, H. Hao, J. Yu, J. Liu, J. Lu, G. Wan, S. He, K. Li, Y. Luo, Chem. Eng. J., 2017, 317, 60-69.
[7] D. He, L. Zhang, Y. Zhao, Y. Mei, D. Chen, S. He, Y. Luo, Environ. Sci. Technol, 2018, 52, 3669-3675.